RESEARCH ARTICLE

PhdA Catalyzes the First Step of Phenazine-1-Carboxylic Acid Degradation in *Mycobacterium fortuitum*

Kyle C. Costa,[a] Leon S. Moskatel,[a*] Lucas A. Meirelles,[a] (ID) Dianne K. Newman[a,b]

[a]Division of Biology and Biological Engineering, California Institute of Technology, Pasadena, California, USA
[b]Division of Geological and Planetary Sciences, California Institute of Technology, Pasadena, California, USA

ABSTRACT Phenazines are a class of bacterially produced redox-active metabolites that are found in natural, industrial, and clinical environments. In *Pseudomonas* spp., phenazine-1-carboxylic acid (PCA)—the precursor of all phenazine metabolites—facilitates nutrient acquisition, biofilm formation, and competition with other organisms. While the removal of phenazines negatively impacts these activities, little is known about the genes or enzymes responsible for phenazine degradation by other organisms. Here, we report that the first step of PCA degradation by *Mycobacterium fortuitum* is catalyzed by a phenazine-degrading decarboxylase (PhdA). PhdA is related to members of the UbiD protein family that rely on a prenylated flavin mononucleotide cofactor for activity. The gene for PhdB, the enzyme responsible for cofactor synthesis, is present in a putative operon with the gene encoding PhdA in a region of the *M. fortuitum* genome that is essential for PCA degradation. PhdA and PhdB are present in all known PCA-degrading organisms from the *Actinobacteria*. *M. fortuitum* can also catabolize other *Pseudomonas*-derived phenazines such as phenazine-1-carboxamide, 1-hydroxyphenazine, and pyocyanin. On the basis of our previous work and the current characterization of PhdA, we propose that degradation converges on a common intermediate: dihydroxyphenazine. An understanding of the genes responsible for degradation will enable targeted studies of phenazine degraders in diverse environments.

IMPORTANCE Bacteria from phylogenetically diverse groups secrete redox-active metabolites that provide a fitness advantage for their producers. For example, phenazines from *Pseudomonas* spp. benefit the producers by facilitating anoxic survival and biofilm formation and additionally inhibit competitors by serving as antimicrobials. Phenazine-producing pseudomonads act as biocontrol agents by leveraging these antibiotic properties to inhibit plant pests. Despite this importance, the fate of phenazines in the environment is poorly understood. Here, we characterize an enzyme from *Mycobacterium fortuitum* that catalyzes the first step of phenazine-1-carboxylic acid degradation. Knowledge of the genetic basis of phenazine degradation will facilitate the identification of environments where this activity influences the microbial community structure.

KEYWORDS mycobacteria, PCA, decarboxylases, degradation, phenazines

Secreted metabolites are common in the microbial world, where they play roles in cellular processes such as quorum sensing, signaling, and nutrient acquisition; some additionally act as antimicrobials and inhibit competitors in the environment (1–13). Phenazines are an important class of secreted metabolites named for the three-ringed heterocyclic phenazine cores they share (14). Phenazines are found in clinical, environmental, and industrial settings; for example, in agriculture, phenazines produced by *Pseudomonas* spp. are important in biocontrol, where they protect dryland cereal crops from a variety of fungal and parasitic infections (15–17). The modification and degra-

Address correspondence to Dianne K. Newman, dkn@caltech.edu.

* Present address: Leon S. Moskatel, Department of Medicine, Scripps Mercy Hospital, San Diego, California, USA.

dation of phenazines is thought to make plants more susceptible to disease (18). Phenazine-1-carboxylic acid (PCA) is the precursor of all bacterially derived phenazines and is produced by *Pseudomonas* and *Streptomyces* spp.; consequently, PCA has been a target in several efforts to isolate and characterize phenazine-degrading organisms (18–20).

To date, all known PCA-degrading bacteria belong to either the genus *Sphingomonas* or the suborder *Corynebacterineae* in the *Actinobacteria* (18, 20). While all of these organisms can degrade PCA, *Mycobacterium fortuitum* can also degrade the PCA derivatives pyocyanin (PYO), phenazine-1-carboxamide (PCN), 1-hydroxyphenazine (1-OH-PHZ), and phenazine (20, 21). In addition to bacterial degradation, a variety of fungi modify and detoxify phenazines (22, 23). While the capacity to degrade and modify phenazines is well established and PCA turnover has been documented *in situ* (19), the genes and proteins catalyzing these activities are poorly characterized.

To understand the role of modification and degradation *in situ*, a deeper understanding of the genetic basis of these activities is needed. To date, an ~40-kb genomic region has been identified in *M. fortuitum* that is essential for the degradation of multiple phenazines (20); contained within this genomic region is a demethylase responsible for the conversion of PYO to 1-OH-PHZ (21). Additionally, multiple dioxygenases are thought to be important for degradation in all known PCA-degrading organisms (20, 24–26). Here, we expand the known pathways of degradation by characterizing a UbiD-like decarboxylase that catalyzes the conversion of PCA to phenazine. On the basis of these data and previous genetic experiments, we propose a model for the initial steps in phenazine degradation by *M. fortuitum*.

RESULTS

Phenazine accumulates as an intermediate in PCA degradation by *Mycobacterium fortuitum*. *M. fortuitum* can completely degrade PCA as the sole source of carbon, energy, and nitrogen concomitant with growth (20). Oxygen-dependent dioxygenases are important for the complete degradation of PCA; however, when *M. fortuitum* is incubated under anoxic conditions, PCA is still removed from the medium and phenazine begins to accumulate (Fig. 1A). These data suggest that phenazine is an intermediate in PCA degradation and that the first step of degradation is catalyzed by a decarboxylase (Fig. 1B). In previous work, we identified an ~40-kb region of the *M. fortuitum* genome that harbors all known genes for phenazine degradation (20) and others of unknown function (Fig. 2). Contained within this region are five annotated decarboxylases that were pursued further.

Heterologous expression and mutagenesis identify the genes necessary for PCA decarboxylation to phenazine. To identify the PCA decarboxylase, each of the five annotated decarboxylases whose coding sequences are contained within the phenazine-responsive region of the *M. fortuitum* strain CT6 genome was expressed in *Escherichia coli* BL21(DE3) (27). After induction, only the strain expressing XA26_16650 (NCBI accession number ALI25512) displayed measurable conversion of PCA to phenazine as assessed by high-performance liquid chromatography (HPLC), although with very low activity (Fig. 1C). These data suggest that XA26_16650 is the PCA decarboxylase that catalyzes the first step of degradation in *M. fortuitum*. To test this hypothesis, the homolog of XA26_16650 was deleted from the *M. fortuitum* ATCC 6841 type strain by replacement with a gentamicin resistance cassette. When incubated on agar plates with 1 mM PCA as the sole carbon source, the mutant was incapable of growth, confirming the necessity of XA26_16650 in PCA degradation (Fig. 1D). This growth defect could be complemented by introducing XA26_16650 in *trans* on the replicative vector pSD5 (28).

PCA degradation is catalyzed by a UbiX/UbiD-like decarboxylase system present in all PCA-degrading *Actinobacteria*. XA26_16650 is annotated as a UbiD family decarboxylase. UbiD catalyzes the decarboxylation of 3-polyprenyl-4-hydroxybenzoate to 2-polyprenylphenol in ubiquinone biosynthesis (29). However, ubiquinone is not present in mycobacteria (30), suggesting that the gene encodes another activity.
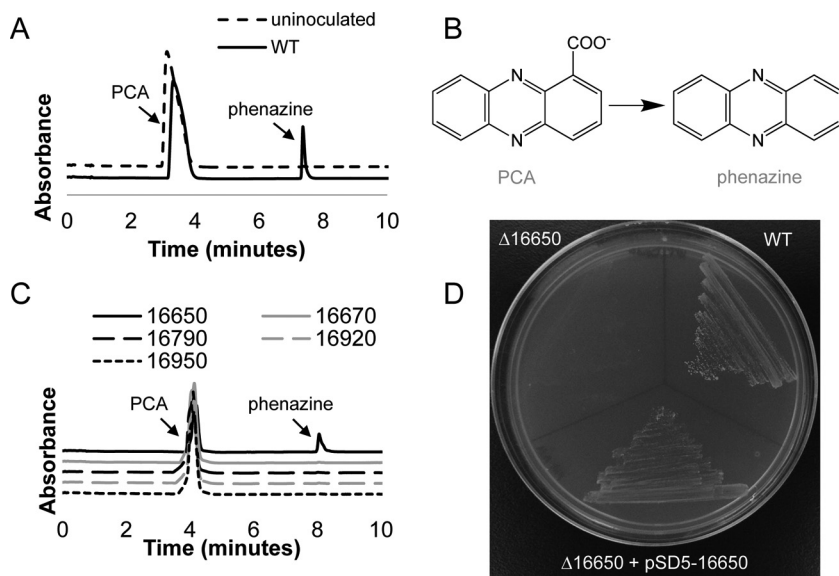
FIG 1 *Mycobacterium fortuitum* catalyzes PCA decarboxylation as the first step in degradation. (A) Cultures of *M. fortuitum* incubated under anoxic conditions and in the presence of PCA catalyzed the formation of phenazine. PCA elutes at around the 4-min mark and phenazine elutes at around the 8-min mark. (B) Proposed reaction catalyzed by *M. fortuitum*. (C) *E. coli* strains expressing individual decarboxylase genes. Phenazine accumulation was only observed in the presence of the *M. fortuitum* gene XA26_16650. (D) *M. fortuitum* lacking the gene XA26_16650 cannot grow on medium with PCA provided as the sole carbon source. When the mutation is complemented in *trans* (+pSD5-16650), growth is restored.

Therefore, we hypothesize that the protein functions as a PCA decarboxylase, here referred to as phenazine-degrading decarboxylase (PhdA). UbiD family decarboxylases utilize a prenylated flavin mononucleotide (prFMN) cofactor in their active site, which is synthesized by the associated cofactor synthase, UbiX. Consistent with this pattern, there is a UbiX homolog (XA26_16670 [NCBI accession number ALI25514]), here referred to as PhdB, whose gene is oriented directly downstream in an operon with the gene encoding PhdA (Fig. 2) (20).

We have identified several *Actinobacteria* capable of PCA degradation (20). Among these, three have sequenced genomes (*M. fortuitum*, *Nocardia* sp. strain LAM0056, and *Rhodococcus* sp. strain JVH1). In all three cases, a PhdA/PhdB system is present on a region of the genome that is syntenic for gene content (Fig. 2). The presence of PhdA/PhdB homologs in each of these organisms, and their absence from close
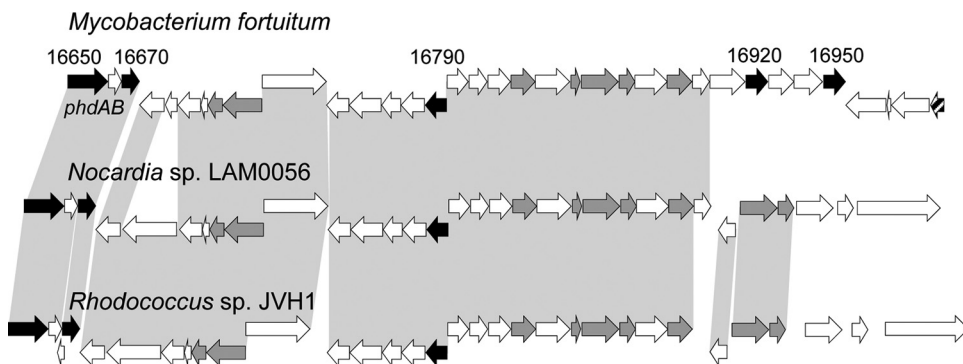

FIG 2 Genomic region responsible for PCA degradation is conserved in different species. The genomic region contains genes encoding dioxygenases (gray), decarboxylases (black), and a pyocyanin demethylase (PodA; striped). Most of the genes from *M. fortuitum*, including PhdA, are conserved in the PCA degraders *Rhodococcus* sp. JVH1 and *Nocardia* sp. LAM0056. Genes that are conserved across genomes are indicated with gray shading.
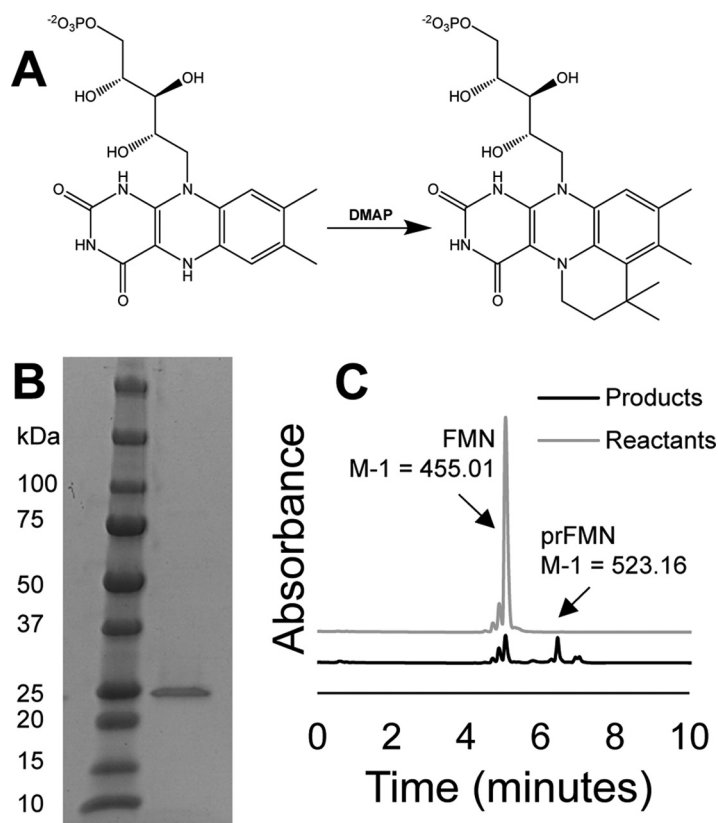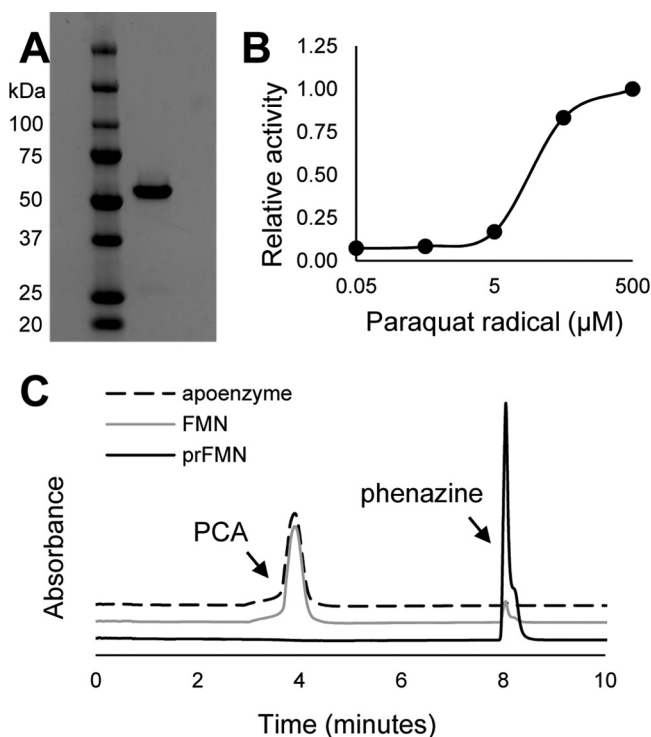
FIG 4 Reaction catalyzed by PhdA. (A) SDS-PAGE gel showing purified PhdA protein. (B) PhdA is only active when incubated with paraquat radical. Protein was incubated for 10 min with paraquat radical at concentrations ranging from 50 nM to 0.5 mM before the addition of 1 mM PCA and displayed a dose-dependent response in activity. (C) PhdA catalyzes the conversion of PCA to phenazine only when reconstituted with the prFMN cofactor. FMN cannot act as a cofactor for the protein.

At pH 7, phenazines are unstable in their radical form and exist primarily in their oxidized and reduced forms (33); however, the paraquat radical is relatively stable at neutral pH (34). Therefore, we hypothesized that the paraquat radical would activate the enzyme when supplied in the reaction mixture. This proved to be the case (Fig. 4B). Because the prFMN cofactor of UbiD-like proteins is sensitive to overoxidation (32), we assume that a radical is necessary to achieve the proper oxidation state. More work is necessary to test this or determine if the paraquat radical could activate other members of the UbiD family that are poorly active when fully oxidized (32).

PhdA displayed robust activity only when reconstituted with prFMN. PhdA mixed with FMN had little activity and the apoprotein was inactive (Fig. 4C). The protein was maximally active at pH 6.9 and in 5% glycerol with no added salt. Under optimal buffering conditions, the holoenzyme had an apparent K_m of 31.2 ± 6.3 μM and k_{cat} of 82.6 ± 33.5 min^{-1} (means $\pm$ standard deviations, $n = 3$).

DISCUSSION

We have identified two genes from *M. fortuitum* that are responsible for the decarboxylation of PCA to phenazine, the essential first step in the degradation pathway. PhdA is a member of the UbiD family of decarboxylases, and PhdB is the required prFMN cofactor synthase. At least three genera (*Mycobacterium*, *Rhodococcus*, and *Nocardia*) in the *Actinobacteria* contain members capable of PCA degradation on the basis of phenotypic analyses and the presence of PhdA and PhdB homologs in their genomes (Fig. 2). Interestingly, while some *Proteobacteria* can degrade PCA, the pathways they utilize for this activity appear distinct from those in the actinobacterial phenazine degraders identified to date. The fact that the genes important for PCA degradation in *M. fortuitum* are also present in other actinobacterial PCA-degrading organisms, and absent from those that lack this activity, further supports the notion that phenazine degradation is catalyzed by a conserved set of genes.

Members of the genus *Sphingomonas* lack *phdA* but still catabolize PCA (18). Biochemical data suggest that this organism may possess a dioxygenase that directly hydroxylates PCA to dihydroxyphenazine (24). However, *in vivo* work suggests that *Sphingomonas* incompletely degrades PCA to 4-hydroxy-1-(2-carboxyphenyl) azacyclobut-2-ene-2-carbonitrile and 4-hydroxy-1-(2-carboxyphenyl)-2-azetidinecarbonitrile (25). These intermediates can only arise when the carboxylate group of PCA is left intact during degradation. Thus, an elucidation of the true pathway of PCA degradation in sphingomonads will require further research; it may be that several enzymes in *Sphingomonas* act on PCA. In any case, it is clear that sphingomonads lack homologs of PhdA.

While several genera of *Actinobacteria* are capable of PCA degradation, we have only observed the degradation of additional phenazines like PYO, PCN, and 1-OH-PHZ in *Mycobacterium* spp. (20). We found that an amidase is likely responsible for the conversion of PCN to PCA (20); further decarboxylation of PCA by PhdA yields phenazine as a product. *M. fortuitum* grows with phenazine as a sole source of nitrogen, confirming that this compound is readily degraded (20). Several ring-hydroxylating dioxygenases are essential for growth with phenazines as a sole carbon source (20); it is likely that one of these acts on phenazine to form phenazine dihydrodiol, which is converted to dihydroxyphenazine through the action of a diol dehydrogenase and further degraded through the action of additional ring-hydroxylating and ring-cleaving dioxygenases. PYO is demethylated by pyocyanin demethylase (PodA) to yield 1-OH-PHZ as a product (21). Genetic evidence suggests that 1-OH-PHZ may be hydroxylated via monooxygenase activity to yield dihydroxyphenazine (20), but biochemical experiments are necessary to validate this prediction.

Thus far, we have not been able to detect intermediates in phenazine degradation by analyzing culture supernatants; however, our genetic and biochemical data lead us to hypothesize that the degradation of several phenazines by *Mycobacterium* spp. converges on dihydroxyphenazine as a catabolic intermediate. In previous work, we reported the XA26_16730 dioxygenase to be important for the degradation of PCA, because a mutant of this gene could not utilize PCA as a carbon source and accumulated a phenazine in culture supernatants (20). Therefore, we hypothesize that XA26_16730 (NCBI accession number ALI25520) is the dioxygenase that acts on phenazine to form phenazine dihydrodiol. The putative operon that contains XA26_16730 also encodes a diol dehydrogenase (XA26_16700) that may be responsible for converting phenazine dihydrodiol to dihydroxyphenazine. These observations lead us to propose a model of the degradation pathway where PCN, PCA, PYO, and 1-OH-PHZ converge on dihydroxyphenazine as a common intermediate (Fig. 5). Future work will test this model of phenazine degradation. The genes identified herein provide a starting point for tracking the presence of phenazine-degrading bacteria in nature, which may facilitate measurements of phenazine turnover in the environment.

MATERIALS AND METHODS

Strains, medium, and culture conditions. The strains, plasmids, and primers used in this study are listed in Table 1. For routine cultivation, all strains were grown in LB medium (Difco). Where appropriate, either carbenicillin (100 μg · ml^{-1}), chloramphenicol (34 μg · ml^{-1}), or gentamicin (100 μg · ml^{-1}) was included. For medium with PCA as the sole carbon source, *M. fortuitum* was grown in minimal medium with 2 mM PCA (liquid medium) or on plates with 1% Noble agar and 1 mM PCA (20). *E. coli* strains were grown at 37°C with shaking at 200 rpm, and *M. fortuitum* was grown at 30°C with shaking at 200 rpm. PCA was purchased from Princeton Biomolecular Research.

To assess the ability of *E. coli* heterologous expression strains to decarboxylate PCA, *E. coli* BL21 carrying each gene on the replicative vector pET-20b(+) or pET-11a was grown to an optical density at 600 nm (OD$_{600}$) of ~0.5 on LB medium and induced with 200 μM IPTG (isopropyl-β-D-thiogalactopyranoside) for 3 h at 30°C. After induction, PCA was added to a final concentration of 100 μM, and cells were incubated for an additional 2 h. Cells were removed by centrifugation, and filtered supernatants were analyzed by HPLC. *E. coli* Rosetta expressing His-tagged XA26_16650 and XA26_16670 was grown overnight to stationary phase in LB medium before transferring (1/1,000 dilution) to 1 liter of LB medium. Cultures were grown for 5 h at 37°C before induction at 30°C with 100 μM IPTG for 3 h. Cell pellets were collected by centrifugation and stored at −80°C for up to 3 months before protein purification.
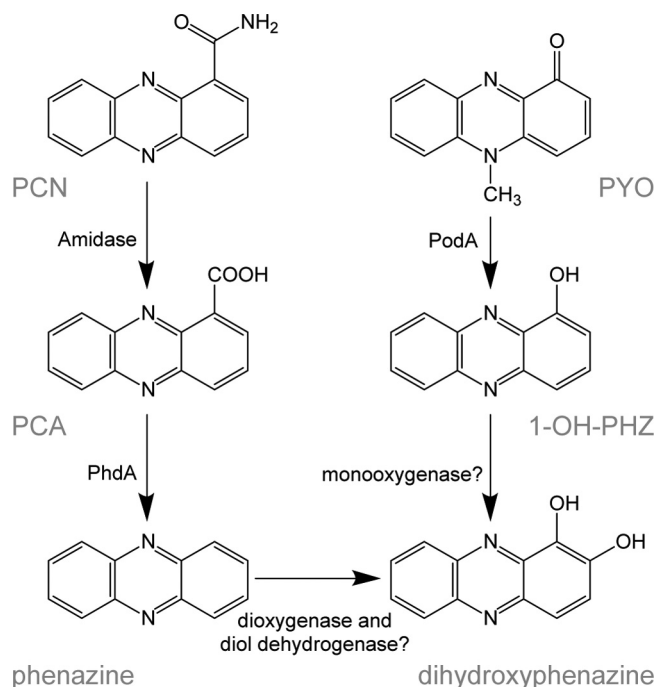
FIG 5 Proposed pathway for the first steps in phenazine degradation by *M. fortuitum*. PYO, 1-OH-PHZ, PCN, and PCA converge on dihydroxyphenazine as a common intermediate. Dihydroxyphenazine is likely further degraded through the action of multiple ring-cleaving and ring-hydroxylating dioxygenases.

Nocardia sp. strain LAM0056 was isolated by inoculating 3 ml of *Nocardia* PCA medium with 30 mg of soil collected from the California Institute of Technology campus and incubating at 30°C. *Nocardia* PCA medium contained 17.1 mM NaCl, 1.97 mM MgCl$_2$·6H$_2$O, 0.68 mM CaCl$_2$·2H$_2$O, 6.71 mM KCl, 20 mM phosphate buffer (KH$_2$PO$_4$-KHPO$_4$ [pH 7]), 1 mM Na$_2$SO$_4$, 10 mM NH$_4$Cl, 1 mM PCA, and trace elements and vitamin solutions (35). Cultures were incubated for 1 to 2 weeks over 3 serial transfers before streak isolation on LB agar medium. DNA was extracted as described previously (20, 36) and sequenced by SMRT sequencing using the Pacific Biosciences RS II platform. *De novo* genome assembly (37) resulted in 5 contigs. The genome was uploaded to the Integrated Microbial Genomes Web server for storage and annotation (https://img.jgi.doe.gov/) under genome identification number 2681813501.

Generation of mutants and heterologous expression strains. For heterologous expression, the gene of interest was PCR amplified using primers listed in Table 1, digested with NdeI, NotI, NheI, or BglII (New England BioLabs), and ligated into the expression vector pET-20b(+) or pET-11a. Plasmids were transformed into either *E. coli* BL21 or Rosetta (Novagen) by electroporation and maintained using antibiotic selection. *M. fortuitum* ATCC 6841 ΔMFORT_16229 (ΔXA26_16650 Δ*phdA*) was generated using a recombineering procedure as described previously (28, 38, 39). Briefly, PCR products for the genomic regions flanking MFORT_16229 were ligated to the gentamicin resistance cassette from pMQ30 (40). This linear construct was electroporated into acetamide-induced *M. fortuitum* carrying the plasmid pJV53 (38) as described previously (39). Mutants were selected on gentamicin-containing medium and screened for the gentamicin cassette at the MFORT_16229 genomic locus by PCR.

To complement the MFORT_16229 deletion, the gene was reintroduced in *trans* on the replicative vector pSD5 (28). First, the mutant was cured of pJV53 by serial passage (20). The coding sequence of MFORT_16229 was ligated into the NdeI and PstI (enzymes from New England BioLabs) sites of pSD5, and the resulting construct was electroporated into *M. fortuitum* ΔMFORT_16229. Cultures containing the plasmid were selected on medium containing kanamycin (100 μg · ml^{-1}).

HPLC analysis of small molecules. HPLC analysis was performed on a Waters Alliance e2695 equipped with a 2998 photodiode array detector and an Acquity QDa mass spectrometry detector. To track PCA and phenazine, a gradient of water with 0.1% NH$_4$OH (buffer A) to 80% acetonitrile with 0.1% NH$_4$OH (buffer B) was run on an XBridge C$_{18}$ 3.5-μm (2.1 mm by 50 mm) column. QDa was run with a cone voltage of 5 V and a capillary voltage of 0.8 kV, and analytes were measured at a 367-nm wavelength. Samples were run at a flow rate of 0.3 ml · min^{-1} with a linear gradient from 0 to 100% buffer B for 10 min, 2 min at 100% buffer B, and a reequilibration for 6 min at 0% buffer B. To determine the kinetic parameters for PhdA, samples were loaded on a Beckman System Gold HPLC system equipped with a photodiode array detector and an XBridge phenyl 5-μm (4.6 mm by 250 mm) column; the data were collected at a wavelength of 250 nm. Samples were run at a flow rate of 0.95 ml · min^{-1} and purified with a gradient of water with 0.1% NH$_4$OH (buffer A) to 100% acetonitrile with 0.1% NH$_4$OH (buffer C) using the following method: a linear gradient from 0% to 50% buffer C for 1 min, a linear gradient of 50% to 90% buffer C for 11 min, 90% to 0% buffer C for 1 min, and a reequilibration for 5 min at 0% buffer C.

TABLE 1 Strains and primers used in this study

Strain or primer	Description or sequence
Strains	
M. fortuitum strain CT6	Wild-type *M. fortuitum*, DNA used for heterologous expression
M. fortuitum ATCC 6841	Wild-type *M. fortuitum*, type strain
M. fortuitum Δ*phdA*	ATCC 6841 with an in-frame deletion of *phdA* (XA26_16650)
M. fortuitum Δ*phdA*(pSD5-*phdA*)	ATCC 6841 with an in-frame deletion of *phdA* (XA26_16650) and *phdA* complemented in *trans*
Nocardia sp. LAM0056	Wild type
E. coli Rosetta/pET-20b(+)-*phdA-His*	Expression construct to generate PhdA-His protein
E. coli Rosetta/pET-20b(+)-*phdB-His*	Expression construct to generate PhdB-His protein
E. coli BL21(DE3)/pET-20b(+)-16650	Expression construct
E. coli BL21(DE3)/pET-20b(+)-16670	Expression construct
E. coli BL21(DE3)/pET-20b(+)-16790	Expression construct
E. coli BL21(DE3)/pET-11a-16920	Expression construct
E. coli BL21(DE3)/pET-20b(+)-16950	Expression construct
Primers	
Expression	
16650-NdeI-F	AAAACATATGGCGGTTTTCCGTGACTTGCGGCATTACATCGACA
16650-NotI-R	TTTTGCGGCCGCTCAGAGCGGCAATGTCGCCTTCCACCGATCGCGGA
16670-NdeI-F	AAAACATATGCGCATCATCGTCGCGATCAGCGGCGCCA
16670-NotI-R	TTTTGCGGCCGCCTACTCGGTGCCGGCAGCTTGA
16790-NdeI-F	AAAACATATGAACATCGAATTCAGCACCGTAATCCAGCCCA
16790-NotI-R	TTTTGCGGCCGCTCAGCAGGCCAGGGTGACGGACCTCAGCGA
16920-NheI-F	AAAAATGGCTAGCCCTGAACACAGTTCACCGATCGCAAGGGCGTTACT
16920-BglII-R	TTTTAGATCTTCATCCTTCTCCGTCAGCAGCGAAACAT
16950-NdeI-F	AAAACATATGACCAGCGCAACGCAGTGGAGTGTCTCGA
16950-NotI-R	TTTTGCGGCCGCCTACTCCGCGCGCGAGCGCGACGGTGCCGAGGT
16650-His-NotI-R	AAAAGCGGCCGCTCAATGGTGATGGTGATGGTGGCTCTGGAAGTACAGGT TTTCGGCGAGCGGCAATGTCGCCTTCCACCGATCGCGGA
16670-His-NotI-R	TTTTGCGGCCGCTCAATGGTGATGGTGATGGTGGCTCTGGAAGTACAGGTT TTCGGCCTCGGTGCCGGCAGCTTGACTGAGGTCAT
Δ*phdA*	
phdA-us-F	CGTTTACGTAGTCTGGCGACCGCCCGAGCAGT
phdA-us-R-XbaI	TTTTTCTAGAATGTCCAATAGATGGTTCGGATATCCATCATCCGATTCACA
phdA-ds-F-NotI	AAAAGCGGCCGCCGGGGTCGAGGAAGGTGGAAAGTGATGACGT
phdA-ds-R	CGTATCACGCATCACGGCTGCTCGTATCCCGCGCGGAGT
Complementation	
phdA-F-NdeI	AAAACATATGGGGGGGCTCGGCGCGCAAGGTGGAAGTGCAGAGCCA
phdA-R-PstI	TTTTCTGCAGTCAGAGCGGCAATGTCGCCTTCCACCGATCGCGGATCT

Purification of PhdA and PhdB. Cell pellets of *E. coli* strains were lysed by sonication using a Fisher Scientific 550 Sonic Dismembrator set to four with 5-s pulses at 25-s intervals. Particulate debris was removed by centrifugation at 50,000 × *g* for 20 min, and the supernatants were applied to a HisTrap HP 5-ml nickel column on an ÄKTApurifier fast-performance liquid chromatography (FPLC) system (GE Healthcare). Proteins were eluted in buffers containing 500 mM NaCl, 5% glycerol, and 20 mM Tris (pH 7.2) over a gradient from 20 mM to 500 mM imidazole applied over 10 column volumes. Proteins were concentrated by centrifugation (Amicon Ultra-15 centrifugal filters, Ultracel 10 K molecular weight cutoff [MWCO]) as necessary. Proteins were used the same day they were purified for subsequent analysis.

Synthesis of prenylated FMN. Prenylated FMN was synthesized using purified XA26_16670-His (PhdB-His), reduced FMN, and dimethylallyl monophosphate (DMAP). DMAP was synthesized from 3-methyl-2-buten-1-ol and tetrabutylammonium phosphate (Sigma) as described previously (41). Fractions with DMAP were identified by thin-layer chromatography and molybdate reagent. Trace tetrabutylammonium phosphate contaminant was removed by ion exchange across an Amberlite IR120 hydrogen form resin that was prewashed with 75% ammonium hydroxide, equilibrated with 100 mM ammonium bicarbonate, and eluted with 100 mM ammonium bicarbonate. DMAP was recovered by lyophilization as a white powder. Purified PhdB-His was mixed with 2.5 mM reduced FMN (reduced with a 4-fold molar excess of sodium dithionite) and a 2-fold molar excess of DMAP under anaerobic conditions (Coy glove box with a 5% H_2-95% N_2 atmosphere) in a buffer consisting of 500 mM NaCl, 5% glycerol, and Tris (pH 7) (32). The reaction mixture was left to incubate for 3 h and monitored by HPLC until at least 90% of the FMN was converted to prFMN. The synthesized prFMN product was separated from PhdB-His by filtration through a 10 K MWCO membrane (Microcon Ultracel YM-10 regenerated cellulose) and assumed to be present at a 2.5 mM concentration in subsequent experiments.

Decarboxylation of PCA by PhdA. PhdA was reconstituted with prFMN under anoxic conditions in a buffer containing 500 mM NaCl, 5% glycerol, Tris (pH 7.2), 1 mM reduced prFMN, 4 mM MnCl₂, and 4 mM KCl (32). After a 10-min incubation, the protein was oxidized by exposure to atmospheric oxygen and buffer exchanged to pH 9.2. Complete oxidation (assessed by visual color change from purple to yellow)

occurred after ~3 h at pH 9.2 (32). To generate the paraquat radical, 10 mM paraquat was mixed with 5 mM sodium dithionite under anoxic conditions. A substoichiometric amount of sodium dithionite was used to avoid the reduction of prFMN in subsequent steps. Reconstituted oxidized PhdA was brought into a Coy anaerobic chamber, added directly (50 to 100 nM final concentration) to buffer containing 5% glycerol, bis-Tris (pH 6.9), and 100 μM paraquat radical, and incubated for 10 min before the addition of various concentrations of PCA (2 to 500 μM). The substrates were mixed with PhdA for 5 min before the reaction was quenched by the addition of NH_4OH (10% final volume). The apparent kinetic parameters for PhdA were determined by monitoring the appearance of phenazine by HPLC. Kinetic parameters were calculated in Excel as previously described (42).

ACKNOWLEDGMENTS

REFERENCES

1. Raymond KN, Müller G, Matzanke BF. 1984. Complexation of iron by siderophores a review of their solution and structural chemistry and biological function, p 49–102. *In* Gutsche DC (ed), Structural chemistry. Topics in current chemistry, vol 123. Springer, Berlin, Germany. https://doi.org/10.1007/3-540-13099-3_2.
2. Hernandez ME, Newman DK. 2001. Extracellular electron transfer. Cell Mol Life Sci 58:1562–1571. https://doi.org/10.1007/PL00000796.
3. Waters CM, Bassler BL. 2005. Quorum sensing: cell-to-cell communication in bacteria. Annu Rev Cell Dev Biol 21:319–346. https://doi.org/10.1146/annurev.cellbio.21.012704.131001.
4. Davies J. 2007. Small molecules: the lexicon of biodiversity. J Biotechnol 129:3–5. https://doi.org/10.1016/j.jbiotec.2006.11.023.
5. Davies J, Ryan KS. 2012. Introducing the parvome: bioactive compounds in the microbial world. ACS Chem Biol 7:252–259. https://doi.org/10.1021/cb200337h.
6. Schuster M, Sexton DJ, Diggle SP, Greenberg EP. 2013. Acyl-homoserine lactone quorum sensing: from evolution to application. Annu Rev Microbiol 67:43–63. https://doi.org/10.1146/annurev-micro-092412-155635.
7. Traxler MF, Kolter R. 2015. Natural products in soil microbe interactions and evolution. Nat Prod Rep 32:956–970. https://doi.org/10.1039/C5NP00013K.
8. Abreu NA, Taga ME. 2016. Decoding molecular interactions in microbial communities. FEMS Microbiol Rev 40:648–663. https://doi.org/10.1093/femsre/fuw019.
9. Fischbach MA, Segre JA. 2016. Signaling in host-associated microbial communities. Cell 164:1288–1300. https://doi.org/10.1016/j.cell.2016.02.037.
10. Papenfort K, Bassler BL. 2016. Quorum sensing signal-response systems in Gram-negative bacteria. Nat Rev Microbiol 14:576–588. https://doi.org/10.1038/nrmicro.2016.89.
11. Springer SD, Butler A. 2016. Microbial ligand coordination: consideration of biological significance. Coord Chem Rev 306:628–635. https://doi.org/10.1016/j.ccr.2015.03.013.
12. Glasser NR, Saunders SH, Newman DK. 2017. The colorful world of extracellular electron shuttles. Annu Rev Microbiol 71:731–751. https://doi.org/10.1146/annurev-micro-090816-093913.
13. Whiteley M, Diggle SP, Greenberg EP. 2017. Progress in and promise of bacterial quorum sensing research. Nature 551:313–320. https://doi.org/10.1038/nature24624.
14. Price-Whelan A, Dietrich LEP, Newman DK. 2006. Rethinking "secondary" metabolism: physiological roles for phenazine antibiotics. Nat Chem Biol 2:71–78. https://doi.org/10.1038/nchembio764.
15. Huang Z, Bonsall RF, Mavrodi DV, Weller DM, Thomashow LS. 2004. Transformation of *Pseudomonas fluorescens* with genes for biosynthesis of phenazine-1-carboxylic acid improves biocontrol of rhizoctonia root rot and in situ antibiotic production. FEMS Microbiol Ecol 49:243–251. https://doi.org/10.1016/j.femsec.2004.03.010.
16. Yang M-M, Mavrodi DV, Mavrodi OV, Bonsall RF, Parejko JA, Paulitz TC, Thomashow LS, Yang H-T, Weller DM, Guo J-H. 2011. Biological control of take-all by fluorescent *Pseudomonas* spp. from Chinese wheat fields.

Phytopathology 101:1481–1491. https://doi.org/10.1094/PHYTO-04-11-0096.
17. Mavrodi DV, Mavrodi OV, Parejko JA, Bonsall RF, Kwak Y-S, Paulitz TC, Thomashow LS, Weller DM. 2012. Accumulation of the antibiotic phenazine-1-carboxylic acid in the rhizosphere of dryland cereals. Appl Environ Microbiol 78:804–812. https://doi.org/10.1128/AEM.06784-11.
18. Yang Z-J, Wang W, Jin Y, Hu H-B, Zhang X-H, Xu Y-Q. 2007. Isolation, identification, and degradation characteristics of phenazine-1-carboxylic acid-degrading strain *Sphingomonas* sp. DP58. Curr Microbiol 55:284–287. https://doi.org/10.1007/s00284-006-0522-7.
19. Mavrodi DV, Parejko JA, Mavrodi OV, Kwak Y-S, Weller DM, Blankenfeldt W, Thomashow LS. 2013. Recent insights into the diversity, frequency and ecological roles of phenazines in fluorescent *Pseudomonas* spp. Environ Microbiol 15:675–686. https://doi.org/10.1111/j.1462-2920.2012.02846.x.
20. Costa KC, Bergkessel M, Saunders S, Korlach J, Newman DK. 2015. Enzymatic degradation of phenazines can generate energy and protect sensitive organisms from toxicity. mBio 6:e01520-15. https://doi.org/10.1128/mBio.01520-15.
21. Costa KC, Glasser NR, Conway SJ, Newman DK. 2017. Pyocyanin degradation by a tautomerizing demethylase inhibits *Pseudomonas aeruginosa* biofilms. Science 355:170–173. https://doi.org/10.1126/science.aag3180.
22. Hill JC, Johnson GT. 1969. Microbial transformation of phenazines by *Aspergillus sclerotiorum*. Mycologia 61:452–467. https://doi.org/10.2307/3757234.
23. Moree WJ, Phelan VV, Wu C-H, Bandeira N, Cornett DS, Duggan BM, Dorrestein PC. 2012. Interkingdom metabolic transformations captured by microbial imaging mass spectrometry. Proc Natl Acad Sci U S A 109:13811–13816. https://doi.org/10.1073/pnas.1206855109.
24. Zhao Q, Hu H-B, Wang W, Huang X-Q, Zhang X-H. 2017. Novel three-component phenazine-1-carboxylic acid 1, 2-dioxygenase in *Sphingomonas wittichii* DP58. Appl Environ Microbiol 83:e00133-17. https://doi.org/10.1128/AEM.00133-17.
25. Chen K, Hu H, Wang W, Zhang X, Xu Y. 2008. Metabolic degradation of phenazine-1-carboxylic acid by the strain *Sphingomonas* sp. DP58: the identification of two metabolites. Biodegradation 19:659–667. https://doi.org/10.1007/s10532-007-9171-1.
26. Ma Z, Shen X, Hu H, Wang W, Peng H, Xu P, Zhang X. 2012. Genome sequence of *Sphingomonas wittichii* DP58, the first reported phenazine-1-carboxylic acid-degrading strain. J Bacteriol 194:3535–3536. https://doi.org/10.1128/JB.00330-12.
27. Studier FW, Moffatt BA. 1986. Use of bacteriophage T7 RNA polymerase to direct selective high-level expression of cloned genes. J Mol Biol 189:113–130. https://doi.org/10.1016/0022-2836(86)90385-2.
28. DasGupta SK, Jain S, Kaushal D, Tyagi AK. 1998. Expression systems for study of mycobacterial gene regulation and development of recombinant BCG vaccines. Biochem Biophys Res Commun 246:797–804. https://doi.org/10.1006/bbrc.1998.8724.
29. Jacewicz A, Izumi A, Brunner K, Schnell R, Schneider G. 2013. Structural

insights into the UbiD protein family from the crystal structure of PA0254 from *Pseudomonas aeruginosa*. PLoS One 8:e63161. https://doi.org/10.1371/journal.pone.0063161.

30. Schoepp-Cothenet B, van Lis R, Atteia A, Baymann F, Capowiez L, Ducluzeau A-L, Duval S, ten Brink F, Russell MJ, Nitschke W. 2013. On the universal core of bioenergetics. Biochim Biophys Acta 1827:79–93. https://doi.org/10.1016/j.bbabio.2012.09.005.

31. White MD, Payne KAP, Fisher K, Marshall SA, Parker D, Rattray NJW, Trivedi DK, Goodacre R, Rigby SEJ, Scrutton NS, Hay S, Leys D. 2015. UbiX is a flavin prenyltransferase required for bacterial ubiquinone biosynthesis. Nature 522:502–506. https://doi.org/10.1038/nature14559.

32. Marshall SA, Fisher K, Ni Cheallaigh A, White MD, Payne KAP, Parker DA, Rigby SEJ, Leys D. 2017. Oxidative maturation and structural characterization of prenylated-FMN binding by UbiD, a decarboxylase involved in bacterial ubiquinone biosynthesis. J Biol Chem 292:4623–4637. https://doi.org/10.1074/jbc.M116.762732.

33. Friedheim E, Michaelis L. 1931. Potentiometric study of pyocyanine. J Biol Chem 91:355–368.

34. Bockman TM, Kochi JK. 1990. Isolation and oxidation-reduction of methylviologen cation radicals. Novel disproportionation in charge-transfer salts by X-ray crystallography. J Org Chem 55:4127–4135.

35. Whitman WB, Shieh J, Sohn S, Caras DS, Premachandran U. 1986. Isolation and characterization of 22 mesophilic methanococci. Syst Appl Microbiol 7:235–240. https://doi.org/10.1016/S0723-2020(86)80012-1.

36. Belisle JT, Mahaffey SB, Hill PJ. 2009. Isolation of mycobacterium species genomic DNA. Methods Mol Biol 465:1–12. https://doi.org/10.1007/978-1-59745-207-6_1.

37. Chin C-S, Alexander DH, Marks P, Klammer AA, Drake J, Heiner C, Clum A, Copeland A, Huddleston J, Eichler EE, Turner SW, Korlach J. 2013. Nonhybrid, finished microbial genome assemblies from long-read SMRT sequencing data. Nat Methods 10:563–569. https://doi.org/10.1038/nmeth.2474.

38. van Kessel JC, Hatfull GF. 2007. Recombineering in *Mycobacterium tuberculosis*. Nat Methods 4:147–152. https://doi.org/10.1038/nmeth996.

39. Goude R, Roberts DM, Parish T. 2015. Electroporation of mycobacteria. Methods Mol Biol 1285:117–130. https://doi.org/10.1007/978-1-4939-2450-9_7.

40. Shanks RMQ, Caiazza NC, Hinsa SM, Toutain CM, O'Toole GA. 2006. *Saccharomyces cerevisiae*-based molecular tool kit for manipulation of genes from Gram-negative bacteria. Appl Environ Microbiol 72:5027–5036. https://doi.org/10.1128/AEM.00682-06.

41. Lira LM, Vasilev D, Pilli RA, Wessjohann LA. 2013. One-pot synthesis of organophosphate monoesters from alcohols. Tetrahedron Lett 54:1690–1692. https://doi.org/10.1016/j.tetlet.2013.01.059.

42. Kemmer G, Keller S. 2010. Nonlinear least-squares data fitting in Excel spreadsheets. Nat Protoc 5:267–281. https://doi.org/10.1038/nprot.2009.182.